Published in final edited form as:

*Nature*. 2009 April 9; 458(7239): 725–731. doi:10.1038/nature07782.

# Tumours with PI3K activation are resistant to dietary restriction

**Nada Y. Kalaany**[1,2,3] and **David M. Sabatini**[1,2,3,4]

[1]Whitehead Institute for Biomedical Research, Nine Cambridge Center, Cambridge, Massachusetts 02142, USA.

[2]Howard Hughes Medical Institute, Department of Biology, Massachusetts Institute of Technology, Cambridge, MA 02139, USA.

[3]Koch Institute for Integrative Cancer Research at MIT, 77 Massachusetts Avenue, Cambridge, Massachusetts 02139, USA.

[4]Broad Institute, Seven Cambridge Center, Cambridge, Massachusetts, 02142, USA.

## Abstract

Dietary restriction (DR) delays the incidence and decreases the growth of various types of tumours, but the mechanisms underlying the sensitivity of tumours to food restriction remain unknown. We find that certain human cancer cell lines, when grown as tumour xenografts in mice, are highly sensitive to the anti-growth effects of DR, while others are resistant. Cancer cells that form DR-resistant tumours carry mutations that cause constitutive activation of the PI3K pathway and in culture proliferate in the absence of insulin or IGF1. Substitution of an activated mutant allele of PI3K with wild-type PI3K in otherwise isogenic cancer cells, or the restoration of PTEN expression in a *PTEN*-null cancer cell line, is sufficient to convert a DR-resistant tumour into one that is DR-sensitive. DR does not affect a *PTEN*-null mouse model of prostate cancer, but significantly decreases tumour burden in a mouse model of lung cancer lacking constitutive PI3K signaling. Thus, the PI3K pathway is a major determinant of the sensitivity of tumours to DR and activating mutations in the pathway may influence the response of cancers to DR-mimetic therapies.

### Key genes/proteins

insulin; IGF-1; PI3K; PTEN; RAS; Akt; FOXO; caspase-3; Ki-67

The life-prolonging anti-tumorigenic effects of dietary restriction (DR) were first described in the beginning of the twentieth century1–3. To date, reports indicate that the incidence as well as growth rates of various types of tumours are reduced in laboratory rodents



Correspondence and requests for materials should be addressed to D.M.S (sabatini@wi.mit.edu).

**Author Contributions** DMS and NYK conceived the project and designed the experiments. NYK performed the experiments. The manuscript was written by NYK and edited by DMS.

undergoing DR, the latter being achieved through a 10 to 50% decrease in caloric intake4–11. Interestingly, the effects of DR are not uniform, with tumours from different tissues responding to restriction to different degrees, and a fraction of tumours originating in the same tissues being resistant to DR4,7,10–14.

A consistent response of animals to DR is a reduction in the levels of circulating factors influencing cellular and organismal growth, notably insulin and insulin-like growth factor-1 (IGF-1)8,11,12,15,16. Despite the common systemic changes that accompany DR and its general anti-tumorigenic effects, the question of whether all tumours, under similar experimental conditions, respond equally to DR remains unanswered. Here, we investigate the responsiveness of different types of human and mouse tumours to DR. We identify the activation status of the PI3K pathway as a molecular signature that largely predicts the sensitivity of a tumour to DR and show that by modulating PI3K activation we can convert a DR-resistant tumour into one that is DR-sensitive.

## Differential sensitivities of tumour xenografts to DR

To investigate the responsiveness of different types of tumours to DR, we injected six established human cancer cell lines derived from the brain (U87-MG), colon (SW620), prostate (PC3) and breast (MDA-MB-231, MDA-MB-435, MCF10DCIS.com17, hereafter MCF10DCIS) subcutaneously into NOD/SCID (non-obese diabetic, severe combined immunodeficient) mice. MDA-MB-231 and MCF10DCIS cells were also injected orthotopically into the mammary fat pads of the mice. Xenograft-bearing mice were then fed ad-libitum a standard rodent diet for 3–4 days (20 days in the case of U87-MG and orthotopic MDA-MB-231), after which they were subdivided into AL (ad-libitum-fed) or DR (dietary-restricted) groups for two to three weeks. All DR mice received daily meals amounting to 60% of the caloric intake of their AL counterparts (i.e., 40% DR), and underwent similar decreases in body weight (20–30%) at the end of the restriction period (Supplementary Fig. 1a, b). In contrast, the tumours formed displayed differential sensitivities to DR and could be classified into two main categories: DR-sensitive tumours, which showed significant decreases in tumour volume (MDA-MB-435, MDA-MB-231 and SW620) and DR-resistant tumours, that grew to similar sizes in AL and DR mice (PC3, U87-MG and MCF10DCIS) (Fig. 1a and Supplementary Fig. 1g). As with their subcutaneous counterparts, DR caused a significant reduction in the volume of orthotopically generated MDA-MB-231 tumour xenografts, whereas MCF10DCIS tumours were completely resistant to DR (Fig. 1b). Consistent with earlier reports15,16, in response to DR all mice experienced notable decreases in plasma levels of insulin and IGF-1 (Supplementary Fig. 1c–f). These findings suggest that factors other than systemic changes in the host underlie the differential sensitivities of the tumour xenografts to DR.

## Constitutive PI3K signaling in DR-resistant tumours

Because the xenografted tumours responded differentially to DR despite similar decreases in insulin and IGF-1 levels, we determined whether the six cancer cell lines studied have differential requirements for these factors for their growth in tissue culture. Indeed, in cell lines that form DR-sensitive tumours (MDA-MB-231, MDA-MB-435, and SW620) insulin

or IGF-1 caused a dose-dependent increase in cell numbers (Fig. 2a). In contrast, cell lines that generate DR-resistant tumours (MCF10DCIS, U87-MG, PC3) grew in culture in an insulin and IGF-1-independent fashion (Fig. 2b).

These results suggested that the cancer cell lines forming DR-resistant tumours have a deregulation in an insulin/IGF-1activated signaling pathway, with the phosphatidylinositol 3-kinase (PI3K)/Akt pathway18 being an attractive candidate. Acting through receptor tyrosine kinases, insulin and IGF-1 recruit PI3K to the cell membrane19, where its activity, which is antagonized by the PTEN (phosphatase and tensin homolog deleted on chromosome 10) tumour suppressor, leads to the recruitment and activation of Akt, a serine/threonine kinase. In turn, Akt phosphorylates and regulates numerous targets that enhance cellular growth and inhibit apoptosis. Consistent with a deregulation in PI3K signaling in cell lines that form DR-resistant tumours, serum withdrawal for 1 or 24 hours did not affect Akt S473 phosphorylation, a marker of Akt activation, in MCF10DCIS, PC3, and U87-MG cells but did in MDA-MB-231, MDA-MB-435, and SW620 cells (Fig. 2c).

Analysis of PTEN expression showed that PTEN loss could account for the serum-insensitive Akt activity20 in PC3 and U87-MG, but not, MCF10DCIS cells (Fig. 2d). Activating mutations in the *PIK3CA* gene, which encodes the catalytic subunit of PI3K, also lead to constitutive Akt activity in cancer cells21–24. By sequencing in all the cell lines exons 9 and 20 of *PI3KCA* that can be the sites of the “hot-spot” E545K and H1047R mutations21,25, respectively, we found that the MCF10DCIS cells harbor a previously unknown H1047R mutation. None of the cell lines that form DR-sensitive tumors have lost PTEN function or carry PI3K activating mutations26 (Fig. 2e). Furthermore, no other common oncogene-activating (e.g. *RAS*, *BRAF*) or tumour suppressor-inactivating (e.g. *TP53*) mutation correlated with tumour cell sensitivity to insulin/IGF-1 in vitro or tumour sensitivity to DR in vivo26 (Fig. 2e). Although PI3K can be directly activated by ras27 and this is necessary for the initiation of ras-driven tumours28, the MDA-MB-231 and SW620 cell lines carrying activated *RAS* alleles form DR-sensitive tumors (Fig. 2e). These results imply that tumour resistance to DR correlates with constitutive activation (e.g. through *PIK3CA* mutations or PTEN loss), rather than hyperactivation of the PI3K pathway.

## DR increases apoptosis in DR-sensitive tumours

While phospho-S473 Akt could not be detected in DR-sensitive tumours by immunohistochemistry, it was readily detected in DR-resistant tumours and its levels did not decrease upon DR (data not shown). Thus, to assay for changes in PI3K signaling in DR-sensitive tumours upon restriction, we examined the FOXO1 transcription factor, a major downstream target of Akt that is selectively phosphorylated as a result of PI3K activation21. Phosphorylation of FOXO1 by Akt leads to its cytoplasmic sequestration and degradation so that a decrease in Akt signaling causes relocalization of FOXO1 to the nucleus, where it induces transcription of pro-apoptotic and anti-proliferative genes29. In the DR-resistant (PC3 and MCF10DCIS) tumours, FOXO1 was predominantly localized to the cytoplasm of tumour cells in both AL and DR mice (Supplementary Fig. 2a, b). In contrast, DR caused a significant re-localization of FOXO1 from the cytoplasm to the nucleus in the cells of DR-

sensitive tumours (MDA-MB-435, SW620 and MDA-MB-231) (Supplementary Fig. 2a, b), indicating that in these tumours DR inhibited PI3K signaling.

Suppression by DR of the growth of DR-sensitive tumours could be the result of enhanced cellular death, decreased cellular proliferation, or both. To distinguish amongst these possibilities, we measured the number of tumour cells that were proliferating or undergoing apoptosis by assaying for Ki-67 and caspase-3 cleavage, respectively. Although DR tended to decrease the number of Ki-67 positive cells in DR-sensitive but not DR-resistant tumours, these effects did not reach statistical significance (data not shown). However, a common apoptotic response to DR was observed in all DR-sensitive, but not -resistant tumour xenografts (Supplementary Fig. 2c, d), correlating with the presence of nuclear FOXO1 in DR-sensitive tumours (Supplementary Fig. 2a, b). Indeed, whereas PC3 tumours maintained low levels of apoptosis under ad-libitum or DR conditions, MDA-MB-435 tumours increased cellular apoptotic rates by 5.6-fold (from 7% to 39%; $p = 0.003$) and SW620 tumours showed massive DR-induced apoptosis, which occurred at the edges of tumours (21.3-fold increase, from 2% to 42.5%;) and also at their centers (2.9-fold increase, from 30.7% to 88.8%) averaging to a 3.6-fold increase (from 18.4% to 65.6%; $p = 0.0003$) in whole tumours (Supplementary Fig. 2c). In orthotopic MCF10DCIS and MDA-MB-231 xenografted tumours, no obvious apoptosis was noted following 12 days of DR (data not shown). Nevertheless, when these tumours were harvested only 2 days following restriction, a significant 6-fold increase in apoptosis was observed in MDA-MB-231 (1.1 to 6.6%; $p = 0.05$) but not in MCF10DCIS tumours (Supplementary Fig. 2d), indicating that in MDA-MB-231 tumours, sensitivity to DR-induced apoptosis occurs at earlier stages of the tumorigenic process. Hence, these analyses show that decreased PI3K signaling in human tumour xenografts correlates with DR-induced apoptosis.

## Conversion of a DR-resistant tumour into one that is DR-sensitive

The correlation between tumour sensitivity to DR and the activation status of the PI3K pathway led us to hypothesize that constitutive PI3K signaling in tumour cells is sufficient to decrease the sensitivity of tumours to DR. To begin testing this idea, we used two cell lines derived from the DLD-1 colorectal cancer cell line21. These cells are isogenic except that one carries a wild-type (DLD-WT) and the other (DLD-Mut) a constitutively active mutant allele (E545K) of *PIK3CA*. Consistent with their genetic statuses, DLD-Mut but not DLD-WT cells maintained high levels of phospho-S473 Akt upon serum withdrawal for 1 or 24 hours (Fig. 3a). The growth responses of the DLD-Mut and DLD-WT cells in culture to increasing concentrations of insulin or IGF-1 (Fig. 3b, c) were reminiscent of those of the cancer lines that form DR-resistant and DR-sensitive tumours, respectively (Fig. 2).

In xenograft studies, subcutaneous injection in NOD/SCID mice of $0.6 \times 10^6$ DLD-WT or $0.25 \times 10^6$ DLD-Mut cells, yielded tumours of approximately equal volume in 18 days (Fig. 3d). Application of a 14-day DR regimen to xenografted mice 4 days following tumour cell injection resulted in DLD-WT tumours that were 2.7-fold smaller in volume than those in AL mice (Fig. 3d). Although DLD-Mut tumours grew at a faster rate than DLD-WT tumours, they showed no significant decrease in tumour size upon DR (Fig. 3d). Analysis of FOXO1 in the DLD1 tumours showed significant re-localization of FOXO1 from the

cytoplasm to the nucleus in the DLD-WT tumour cells upon DR (Fig. 4a). FOXO1 remained cytoplasmic in DLD-Mut cells regardless of restriction (Fig. 4a). Furthermore, DLD-WT but not DLD-Mut tumours had a significant enhancement in caspase-3 cleavage (12.5-fold) upon the 14-day DR period (Fig. 4c). Thus, the presence of a PI3K activating mutation in an otherwise DR-sensitive tumour cell line is sufficient to protect tumours formed by these cells from the anti-growth and pro-apoptotic effects of DR.

Because PTEN loss also leads to aberrant PI3K activation20, we investigated the role of PTEN in determining tumour sensitivity to DR. We made use of a *PTEN*-null cell line (U87-MG) that was engineered to induce PTEN expression upon addition of doxycycline30. In culture in vitro, doxycycline-induced PTEN expression caused a decrease in phospho-S473 Akt levels in U87-MG cells (Fig. 3e, left panel) and was sufficient to transform the serum-insensitive U87-MG cells (see Fig. 2c) into serum-sensitive cells that responded to serum withdrawal by decreasing levels of phospho-S473Akt (Fig. 3e, right panel). In contrast to *PTEN*-null U87-MG cells (Fig. 2b), PTEN-expressing U87-MG cells increased their net growth rates in response to increasing levels of insulin and IGF-1 (Fig. 3f).

In vivo doxycycline administration induced PTEN expression in tumour xenografts formed from U87-MG cells (Supplementary Fig. 3a, b). As expected from restoring the expression of a tumour suppressor, the growth rate of U87-MG tumours decreased significantly in the presence of doxycycline, regardless of diet. Nevertheless, the re-expression of PTEN was sufficient to switch the response of U87-MG tumours from being resistant to DR (Fig. 1a and Fig. 3g, left panel) to one that is DR-sensitive (Fig. 3g, right panel). Upon DR, the number of Ki-67 positive cells tended to decrease (by 15%) in PTEN-expressing U87-MG tumours, without, however, reaching statistical significance (data not shown). In the absence of PTEN, FOXO1 was mostly sequestered in the cytoplasm of U87-MG tumour cells in AL as well as DR mice (Fig. 4b). However, upon DR of mice bearing PTEN-expressing U87-MG tumours, FOXO1 re-localized to the nucleus of tumour cells (Fig. 4b), and this correlated with enhanced apoptosis (Fig. 4d), consistent with results obtained for all DR-sensitive tumours (Supplementary Fig. 2 and Fig. 4). Therefore, restoration of PTEN expression in a DR-resistant, *PTEN*-null cancer cell line is sufficient to convert it to a cell line that forms DR-sensitive tumour xenografts in vivo.

## FOXO1 overexpression sensitizes tumours to DR

To investigate the effects of the FOXO factors on the response of tumours to DR, we overexpressed FOXO1 in SW620 cells (Supplementary Fig. 4a) and analyzed the sensitivity to DR of the corresponding tumour xenografts compared to control tumours expressing green fluorescent protein (GFP). A cell line that forms DR-sensitive rather than DR-resistant tumours was used because FOXO1 function is unlikely to be regulated by DR in cancer cells where Akt is constitutively active. FOXO1 overexpression in SW620 xenograft tumours slightly slowed tumour growth (30% decrease) in the AL feeding condition, likely due to aberrant entry of exogenous FOXO1 into the nucleus (Supplementary Fig. 4b). Importantly, in tumours overexpressing FOXO1, DR caused a greater fold reduction in tumour volume (4.1-fold) than in tumours expressing GFP (2.3-fold) (Supplementary Fig. 4b). Immunohistochemical analyses showed that upon DR, FOXO1 localized to the nucleus in

FOXO1-overexpressing as well as control tumours (Supplementary Fig. 4c), particularly in areas that coincided with enhanced caspase-3 cleavage (Supplementary Fig. 4d). Under AL conditions the number of apoptotic cells was slightly enhanced in FOXO1-overexpressing tumours compared to the control tumours. However, the DR-induced apoptotic response increased to a larger extent upon DR in FOXO1-overexpressing tumours than in control tumours (Supplementary Fig. 4d). No significant changes in proliferation were detected among the different tumours (data not shown). These findings are consistent with FOXO1 playing a key role in the anti-tumour effects of DR, but do not preclude the involvement of other PI3K effectors, including other FOXO family members.

## A *PTEN*-null mouse model of prostate cancer is resistant to DR

We next examined the effects of DR in two engineered mouse models of cancer. The first model (*Probasin-Cre; PTEN L/L*) is driven by PTEN loss in the prostate and recapitulates human prostate cancer progression31. The second (*K-RAS$^{LA2}$; P53 LSL/ WT*) is driven by K-ras activation as well as p53 heterozygosity and leads to the development of lung adenocarcinoma32,33. Compared to the AL condition, DR significantly reduced the size of tumour nodules (42% decrease) in the lungs of 7 week-old *K-RAS$^{LA2}$; P53 LSL/ WT* mice (Fig. 5a). Although the lung tumours were of similar pathological grade under both the AL feeding and DR (Fig. 5b), DR strongly decreased the number of proliferating tumour cells (4-fold; 12.5% to 3.1%; $p = 8 \times 10^{-8}$) without affecting the rates of apoptosis (Fig. 5c, d).

In the prostates of 11 week-old *Probasin-Cre; PTEN L/L* mice, DR did not have any detectable effect on the extent or histological appearance of the prostate intraepithelial neoplasia (PIN) (Fig. 5e) or on the activation levels of Akt (Fig. 5f). Indeed, neither the proliferative, nor apoptotic indices of the PIN were affected by DR (Fig. 5g, h). Similar results were obtained in the prostates of 7–8 week-old *Probasin-Cre; PTEN L/L* mice given the same DR regimen (data not shown). Thus, consistent with the human tumour xenograft studies, engineered mouse tumours without mutations that confer constitutive PI3K signaling appear to be DR-sensitive while those with such mutations are DR-resistant.

## Discussion

Dietary restriction (DR) has long been known to suppress tumour growth in laboratory rodents10. We find that genetic alterations in *PIK3CA* or *PTEN* can predict the response of tumours to DR, classifying them into DR-sensitive and DR-resistant tumours. Our results suggest that differential levels of PI3K activation in tumours contribute to their differential sensitivities to DR. It is important to note that we have studied the effects of relatively short-term DR on the growth of tumours at early stages of the tumorigenic process. Thus, at more advanced tumour stages, signaling pathways other than PI3K may play key roles in mediating the effects of DR.

It is interesting to consider which of the downstream effectors of PI3K may mediate the responses of tumours to DR that we have observed. Attractive candidates are the FOXO family of transcription factors that regulate proliferation and apoptosis. Reminiscent of the cell type- and tissue microenvironment-dependent effects of the FOXO factors on

proliferation and apoptosis34, we find that DR causes strong suppression of proliferation in the engineered mouse lung cancer model, while having a prominent pro-apoptotic effect in the human tumour xenograft models. Upon DR, FOXO moves from the cytoplasm to the nucleus only in the cells of DR-sensitive tumours and overexpression of FOXO sensitizes tumours to the anti-growth effects of DR. These results suggest an important role for the FOXO factors but do not exclude potential roles for other PI3K effectors. The activity of signaling molecules that interact at multiple levels with the PI3K pathway, such as mTOR, AMPK, and SIRT1, are likely to fine-tune the sensitivities of tumours to DR (see Supplementary Discussion).

Our findings are consistent with the effects of DR on the growth of early tumours being the result of both systemic changes in the host and signaling events intrinsic to the tumour. These findings should allow for the prediction of the responsiveness of a specific tumour to DR, based on a readily measurable molecular signature, namely the activation status of the PI3K pathway in the tumour cells.

## METHODS SUMMARY

Cell lines were obtained from the Karmanos Cancer Institute (MCF10DCIS.com), B. Vogelstein (DLD-WT and DLD-Mut), M. M. Georgescu (U87-MG) and ATCC (all others) and grown under conditions described by the providers. SW620 cell lines stably overexpressing human FOXO1 or GFP were generated by infection with lentiviruses expressing the corresponding cDNA. Cellular proliferation was measured using the XTT kit (Roche). For immunoblotting, protein lysates were probed with Phospho-S473 Akt, Akt or PTEN antibodies (1:1000, Cell Signaling Technologies). Immunohistochemistry detection of PTEN, FOXO1 and cleaved caspase-3 antibodies (1:100, Cell Signaling Technologies) was performed on paraffin-embedded, sliced tumour sections according to the manufacturer's protocols. PI3K mutations E545K and H1047R were detected by sequencing of two *PIK3CA* fragments amplified by RT-PCR from total RNA extracted from each cell line. All animal studies and procedures were approved by the MIT Institutional Animal Care and Use Committee. Mouse xenografts were generated by injecting tumour cells subcutaneously into male (female for breast cancer cell lines) or orthotopically in the fat pads of female NOD/SCID mice. Five-week-old *K-RAS$^{LA2}$; P53 Lox/Stop/Lox (LSL)/ WT* mice, obtained from the Jacks laboratory32,33 and five-week-old as well as 9-week-old *Probasin-Cre; PTEN Lox/Lox (L/L)* 31 mice were used in the DR studies. DR was achieved by providing individually caged mice a daily portion of a chow diet fortified with vitamins and minerals amounting to 60% of the daily food intake of their ad-libitum-fed counterparts. Mice were euthanized at the beginning of the light cycle, following retro-orbital blood withdrawal. Tumours were harvested, measured and flash-frozen in liquid nitrogen or fixed in formalin. Plasma insulin and IGF-1 levels were determined by ELISA (CrystalChem and Diagnostic Systems Laboratories, respectively). Data are presented as means ± s.e.m., and significant P values ($\leq 0.05$) were obtained by performing non-paired, two-tailed Student's *t* tests to compare two groups.

## METHODS

### Cell lines

MDA-MB-231, MDA-MB-435, PC3 and SW620 cell lines were obtained from ATCC and cultured in DMEM supplemented with 10% FBS. SW620 cell lines stably overexpressing human FOXO1 or GFP were generated by infection with lentiviruses expressing the corresponding cDNA and selected for puromycin resistance (2μg/ml) for 7 days prior to injection into mice. MCF10DCIS.com cell lines were from the Karmanos Cancer Institute and grown in DMEM/F12 with 5% horse serum. The isogenic cell lines DLD-WT and DLD-Mut were from B. Vogelstein and cultured as described21. The doxycycline-inducible U87-MG cell lines were provided by M. M. Georgescu and maintained as described30.

### Proliferation assay

On day 0, cell lines were seeded in their appropriate media in four 96-well plates each, at a density of 3000 (DLD-WT, DLD-Mut and SW620), 5000 (MCF10DCIS, PC3) or 7500 (MDA-MB-231, MDA-MB-435 and U87-MG) cells/well and all plates were incubated overnight. On day 1, three assay plates (for days 3, 5 and 7) of each cell line were washed once with DMEM in the absence of serum and their media were replaced with DMEM supplemented with 0.1% FBS only or with 0.1% FBS and 12 different concentrations of insulin (1, 10, 50, 100, 1000 and 10,000 ng/ml) or IGF-1 (0.5, 5, 25, 50, 100 and 500 ng/ml). Six wells per media condition were used in each plate. The fourth plate from each cell line was used as a baseline day 1 measurement of cell number without addition of the assay media. The cell proliferation kit II (XTT, Roche) was used to measure cell number on days 1, 3, 5 and 7 of the assay.

### Immunoblotting

Cells were rinsed once in ice-cold PBS and harvested in lysis buffer containing 50mM Hepes, pH 7.4, 40mM NaCl, 2mM EDTA, 1.5mM orthovanadate, 50mM NaF, 10mM pyrophosphate, 10mM glycerophosphate, EDTA-free protease inhibitors (Roche) and 1% Triton-X-100. Tumour tissues were homogenized in lysis buffer supplemented with 1% deoxycholate and 0.1% SDS. Proteins from total lysates were resolved by 8–12% SDS-PAGE, and analyzed by immunoblotting as described35 using antibodies for phospho-S473 Akt, Akt and PTEN (1:1000, Cell Signaling Technology).

### DNA sequencing

RNA was extracted and cDNA was prepared from all cell lines as previously described36. Two fragments of the *PIK3CA* (NM_006218) were amplified by PCR that enclosed either the E545K (nucleotide 1573–1996) or the H1047R (nucleotide 3213–3466) PI3K hot-spot mutation21 using primer pairs PIK1-For/PIK3-Rev, or PIK5-For/PIK2-Rev, respectively. PCR conditions were as follows: 95 °C for 3 min, 40 cycles of 94 °C for 30 s, 54 °C (PIK1-For/PIK3-Rev) or 53 °C (PIK5-For/PIK2-Rev) for 30 s, and 68 °C for 30 s (PIK1-For/PIK3-Rev) or 20 s (PIK5-For/PIK2-rev), followed by a final cycle of 68 °C for 10 min. The (PIK1-For/PIK3-Rev) and (PIK5-For/PIK2-Rev) amplified fragments were then purified and sequenced using PIK7-For and PIK2-Rev, respectively.

PIK1-For: 5'-CTTAGAGTTGGAGTTTGACTGG-3'

PIK2-Rev: 5'-CATGGATTGTGCAATTCCTATGC-3'

PIK3-Rev: 5'-ACCTCGAACCATAGGATCTGG-3'

PIK5-For: 5'-TTGCATACATTCGAAAGACC-3'

PIK7-For: 5'-GATTGAAGAGCATGCCAATTG-3'

## Mouse studies

All animal studies and procedures were approved by the MIT Institutional Animal Care and Use Committee. Six- to eight-week-old NOD/SCID mice (from Jackson laboratory) were used for generating all xenografts, with females for breast cancer and males for all other cancer models. In subcutaneous xenografts, mice were injected at two sites in the dorsal region, under isofluorane anesthesia with 100 μl / injection of tumour cell suspension in Hank's Buffered Salt Solution (HBSS, Invitrogen) with 15% matrigel. In orthotopic xenografts, mice were anesthetized with 2,2,2-tribromoethanol, a ventral incision was made in the skin and 25 μl of cell suspension in HBSS with 33% matrigel were injected into the fourth pair of inguinal fat pads. Matrigel used in all experiments was phenol red-free and growth factor-reduced (BD Biosciences). Appropriate tumour cell numbers were injected depending on the tumour growth rates in vivo. For subcutaneous tumours xenografts: $0.25 \times 10^6$ cells for DLD-Mut, $0.5 \times 10^6$ for PC3; $0.6 \times 10^6$ for DLD-WT; $1 \times 10^6$ for MCF10DCIS and SW620; $2 \times 10^6$ for MDA-MB-435 and U87-MG; $2.5 \times 10^6$ for MDA-MB-231. For orthotopic xenografts: $0.1 \times 10^6$ cells for MCF10DCIS and $1 \times 10^6$ for MDA-MB-231.

## Dietary Restriction (DR)

For a period of 3–4 days (20 days for U87-MG and orthotopic MDA-MB-231 xenografts) following injection of tumour cells, all mice were fed an ad-libitum (AL) irradiated rodent chow diet (Prolab RMH 3000, 5P00) providing 3.46 kcal/g physiological fuel value, 26% of which is from protein, 14% from fat and 60% from carbohydrates. All mice were then individually caged and subdivided into an AL group and a 40% DR group. Weekly body weights and daily AL food intake were recorded. Restricted mice received a daily afternoon meal of a DR diet that amounted to 60% of the daily food intake of their AL counterparts. The DR diet has similar consistency to the AL diet except that it is fortified with vitamins and minerals (LabDiet, 5B6V) so as to prevent deficiency in these nutrients in the restricted mice. For U87-MG xenografts, 0.2 mg/ml doxycycline was administered in the drinking water 3 days prior to food restriction and was then replenished three times a week throughout the experiment. DR was carried for 12–15 days (24 days for subcutaneous MCF10DCIS and MDA-MB-231). Five-week-old *K-RAS$^{LA2}$; P53 LSL /WT* mice (obtained from the Jacks laboratory)32,33 and 9-week-old as well as five-week old *Probasin-Cre; PTEN L/L*31 mice of mixed background were used in the DR studies.

### Necropsy and plasma analyses

Mice were euthanized at the beginning of the light cycle following retro-orbital blood withdrawal and plasma was prepared as described36. Plasma insulin and IGF-1were assayed using kits from CrystalChem and Diagnostic Systems Laboratories, respectively. Tumours were harvested, their dimensions (termed a, b and c) were measured with a caliper and tumour volume estimated according to the ellipsoid formula: $4/3 \times \pi \times (a/2 \times b/2 \times c/2)$37. Tumours were then either immediately frozen in liquid nitrogen or fixed in formalin for later processing.

### Immunohistochemistry

Formalin-fixed tumours were embedded in paraffin and sections were immunostained according to the manufacturer's protocol using PTEN (1:100), FOXO1 (1:50) or cleaved caspase-3 (1:100) antibodies, (Cell Signaling Technology). The latter staining was performed using an automated stainer in the Histology Core Laboratory at MIT. Quantification analysis was accomplished by measuring the ratios of cleaved caspase-3-stained cells (visual count) over hematoxylin-stained cells (automated count using CellProfiler program38,39) in an average of 9 pictures of 3 different tumours (1000 nuclei/picture) for each particular xenograft/diet condition.

### Statistical Analysis

Data are presented as means ± s.e.m. In comparing two groups, two-tailed non-paired Student's *t* test was performed and $P \leq 0.05$ (unless otherwise stated) was considered significant.

## Supplementary Material

Refer to Web version on PubMed Central for supplementary material.

## Acknowledgements

We thank B. Vogelstein for providing the isogenic DLD-1 cell lines and M.M. Georgescu for the doxycycline-inducible U87-MG cell line; T. Jacks for the *K-RAS*$^{LA2}$, *P53 LSL/ WT* and H. Wu for the *Probasin-Cre, PTEN L/L* mice; F. Reinhardt for assistance with animal experiments; R. Bronson for histological analysis; the Histology Facility at the Koch Institute for Integrative Cancer Research and the Histology Core Laboratory at MIT for assistance with sectioning and immunohistochemistry; the Imaging Platform at the Broad Institute for assistance with image analysis; R. Weinberg, D. Guertin, Y. Chudnovsky and Y. Sancak for critical reading of the manuscript; and members of the Sabatini and Weinberg labs for support and discussions; This research is supported by the Alexander and Margaret Stewart Trust Award, the David H. Koch Cancer Research Award and NIH grants R01 AI04389 and R01 CA129105. D.M.S. is an investigator of the Howard Hughes Medical Institute.

## References

1. Moreschi C. Beziehung zwischen Ernahrung und Tumorwachstum. Z. Immunitatsforsch. 1909; 2:651–675.
2. Rous P. The influence of diet on transplanted and spontaneous tumors. Exp. Med. 1914; 20:351–413.
3. McCay CM, Crowell MF, Maynard LA. The effect of retarded growth upon the length of life span and upon the ultimate body size. J. Nutr. 1935; 18:63–79.
4. Tannenbaum A, Silverstone H. The influence of the degree of caloric restriction on the formation of skin tumors and hepatomas in mice. Cancer Res. 1949; 9:724–727. [PubMed: 15395906]

5. Tannenbaum A, Silverstone H. Effect of limited food intake on survival of mice bearing spontaneous mammary carcinoma and on the incidence of lung metastases. Cancer Res. 1953; 13:532–536. [PubMed: 13067072]
6. Cheney KE, et al. Survival and disease patterns in C57BL/6J mice subjected to undernutrition. Exp Gerontol. 1980; 15:237–258. [PubMed: 7409023]
7. Weindruch R, Walford RL. Dietary restriction in mice beginning at 1 year of age: effect on life-span and spontaneous cancer incidence. Science. 1982; 215:1415–1418. [PubMed: 7063854]
8. Klurfeld DM, Welch CB, Davis MJ, Kritchevsky D. Determination of degree of energy restriction necessary to reduce DMBA-induced mammary tumorigenesis in rats during the promotion phase. J Nutr. 1989; 119:286–291. [PubMed: 2493082]
9. Zhu Z, Haegele AD, Thompson HJ. Effect of caloric restriction on pre-malignant and malignant stages of mammary carcinogenesis. Carcinogenesis. 1997; 18:1007–1012. [PubMed: 9163688]
10. Kritchevsky D. Caloric restriction and cancer. J Nutr Sci Vitaminol (Tokyo). 2001; 47:13–19. [PubMed: 11349885]
11. Thompson HJ, Zhu Z, Jiang W. Dietary energy restriction in breast cancer prevention. J Mammary Gland Biol Neoplasia. 2003; 8:133–142. [PubMed: 14587868]
12. Sell C. Caloric restriction and insulin-like growth factors in aging and cancer. Horm Metab Res. 2003; 35:705–711. [PubMed: 14710349]
13. Cheney KE, et al. The effect of dietary restriction of varying duration on survival, tumor patterns, immune function, and body temperature in B10C3F1 female mice. J Gerontol. 1983; 38:420–430. [PubMed: 6306089]
14. Pugh TD, Oberley TD, Weindruch R. Dietary intervention at middle age: caloric restriction but not dehydroepiandrosterone sulfate increases lifespan and lifetime cancer incidence in mice. Cancer Res. 1999; 59:1642–1648. [PubMed: 10197641]
15. Ruggeri BA, Klurfeld DM, Kritchevsky D, Furlanetto RW. Caloric restriction and 7,12-dimethylbenz(a)anthracene-induced mammary tumor growth in rats: alterations in circulating insulin, insulin-like growth factors I and II, and epidermal growth factor. Cancer Res. 1989; 49:4130–4134. [PubMed: 2501021]
16. Breese CR, Ingram RL, Sonntag WE. Influence of age and long-term dietary restriction on plasma insulin-like growth factor-1 (IGF-1), IGF-1 gene expression, and IGF-1 binding proteins. J Gerontol. 1991; 46:B180–B187. [PubMed: 1716275]
17. Miller FR, Santner SJ, Tait L, Dawson PJ. MCF10DCIS.com xenograft model of human comedo ductal carcinoma in situ. J Natl Cancer Inst. 2000; 92:1185–1186. [PubMed: 10904098]
18. Manning BD, Cantley LC. AKT/PKB signaling: navigating downstream. Cell. 2007; 129:1261–1274. [PubMed: 17604717]
19. Engelman JA, Luo J, Cantley LC. The evolution of phosphatidylinositol 3-kinases as regulators of growth and metabolism. Nat Rev Genet. 2006; 7:606–619. [PubMed: 16847462]
20. Salmena L, Carracedo A, Pandolfi PP. Tenets of PTEN tumor suppression. Cell. 2008; 133:403–414. [PubMed: 18455982]
21. Samuels Y, et al. Mutant PIK3CA promotes cell growth and invasion of human cancer cells. Cancer Cell. 2005; 7:561–573. [PubMed: 15950905]
22. Kang S, Bader AG, Vogt PK. Phosphatidylinositol 3-kinase mutations identified in human cancer are oncogenic. Proc Natl Acad Sci U S A. 2005; 102:802–807. [PubMed: 15647370]
23. Saal LH, et al. PIK3CA mutations correlate with hormone receptors, node metastasis, and ERBB2, and are mutually exclusive with PTEN loss in human breast carcinoma. Cancer Res. 2005; 65:2554–2559. [PubMed: 15805248]
24. Zhao JJ, et al. The oncogenic properties of mutant p110alpha and p110beta phosphatidylinositol 3-kinases in human mammary epithelial cells. Proc Natl Acad Sci U S A. 2005; 102:18443–18448. [PubMed: 16339315]
25. Samuels Y, et al. High frequency of mutations of the PIK3CA gene in human cancers. Science. 2004; 304:554. [PubMed: 15016963]
26. Cancer Cell Line Project. 1992www.sanger.ac.uk/genetics/CGP/CellLines/

27. Rodriguez-Viciana P, et al. Phosphatidylinositol-3-OH kinase as a direct target of Ras. Nature. 1994; 370:527–332. [PubMed: 8052307]
28. Gupta S, et al. Binding of ras to phosphoinositide 3-kinase p110alpha is required for ras-driven tumorigenesis in mice. Cell. 2007; 129:957–968. [PubMed: 17540175]
29. Calnan DR, Brunet A. The FoxO code. Oncogene. 2008; 27:2276–2288. [PubMed: 18391970]
30. Radu A, Neubauer V, Akagi T, Hanafusa H, Georgescu MM. PTEN induces cell cycle arrest by decreasing the level and nuclear localization of cyclin D1. Mol Cell Biol. 2003; 23:6139–6149. [PubMed: 12917336]
31. Wang S, et al. Prostate-specific deletion of the murine Pten tumor suppressor gene leads to metastatic prostate cancer. Cancer Cell. 2003; 4:209–221. [PubMed: 14522255]
32. Johnson L, et al. Somatic activation of the K-ras oncogene causes early onset lung cancer in mice. Nature. 2001; 410:1111–1116. [PubMed: 11323676]
33. Ventura A, et al. Restoration of p53 function leads to tumour regression in vivo. Nature. 2007; 445:661–665. [PubMed: 17251932]
34. Fu Z, Tindall DJ. FOXOs, cancer and regulation of apoptosis. Oncogene. 2008; 27:2312–2319. [PubMed: 18391973]
35. Kim DH, et al. mTOR interacts with raptor to form a nutrient-sensitive complex that signals to the cell growth machinery. Cell. 2002; 110:163–175. [PubMed: 12150925]
36. Kalaany NY, et al. LXRs regulate the balance between fat storage and oxidation. Cell Metab. 2005; 1:231–244. [PubMed: 16054068]
37. Wapnir IL, Wartenberg DE, Greco RS. Three dimensional staging of breast cancer. Breast Cancer Res Treat. 1996; 41:15–19. [PubMed: 8932872]
38. Carpenter AE, et al. CellProfiler: image analysis software for identifying and quantifying cell phenotypes. Genome Biol. 2006; 7:R100. [PubMed: 17076895]
39. Lamprecht MR, Sabatini DM, Carpenter AE. CellProfiler: free, versatile software for automated biological image analysis. Biotechniques. 2007; 42:71–75. [PubMed: 17269487]

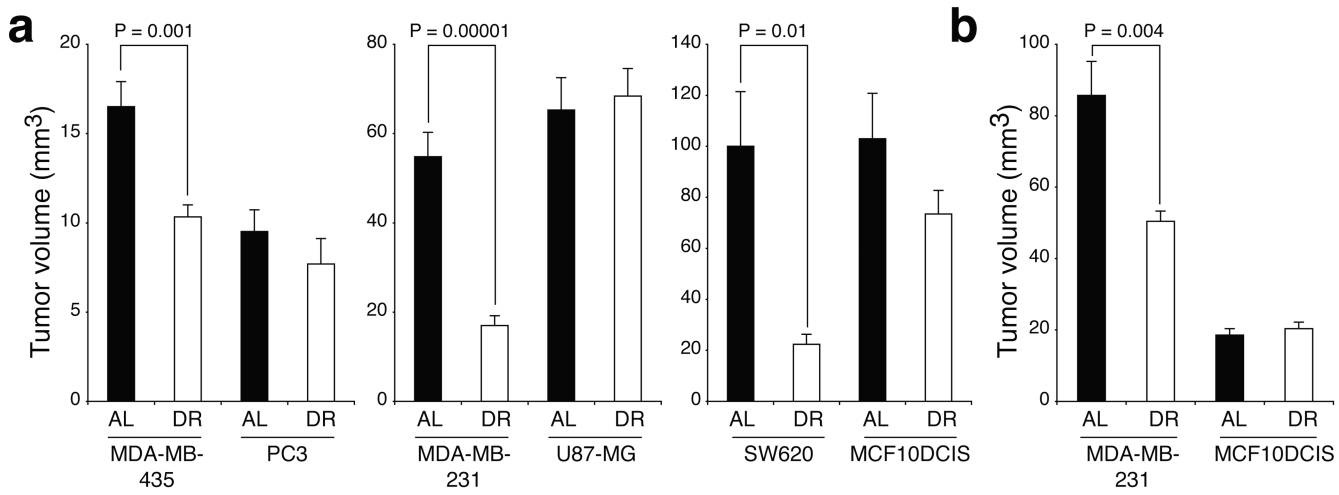


**Figure 1. Human tumour xenografts display differential sensitivities to dietary restriction**

**a,b,** Volumes of six different subcutaneous (a) or two orthotopic human tumour xenografts (b) in NOD/SCID mice that were either ad-libitum fed (AL) or dietary restricted (DR). N= 6 to 12 tumours. Data are means ± s.e.m. * indicates $P < 0.05$.

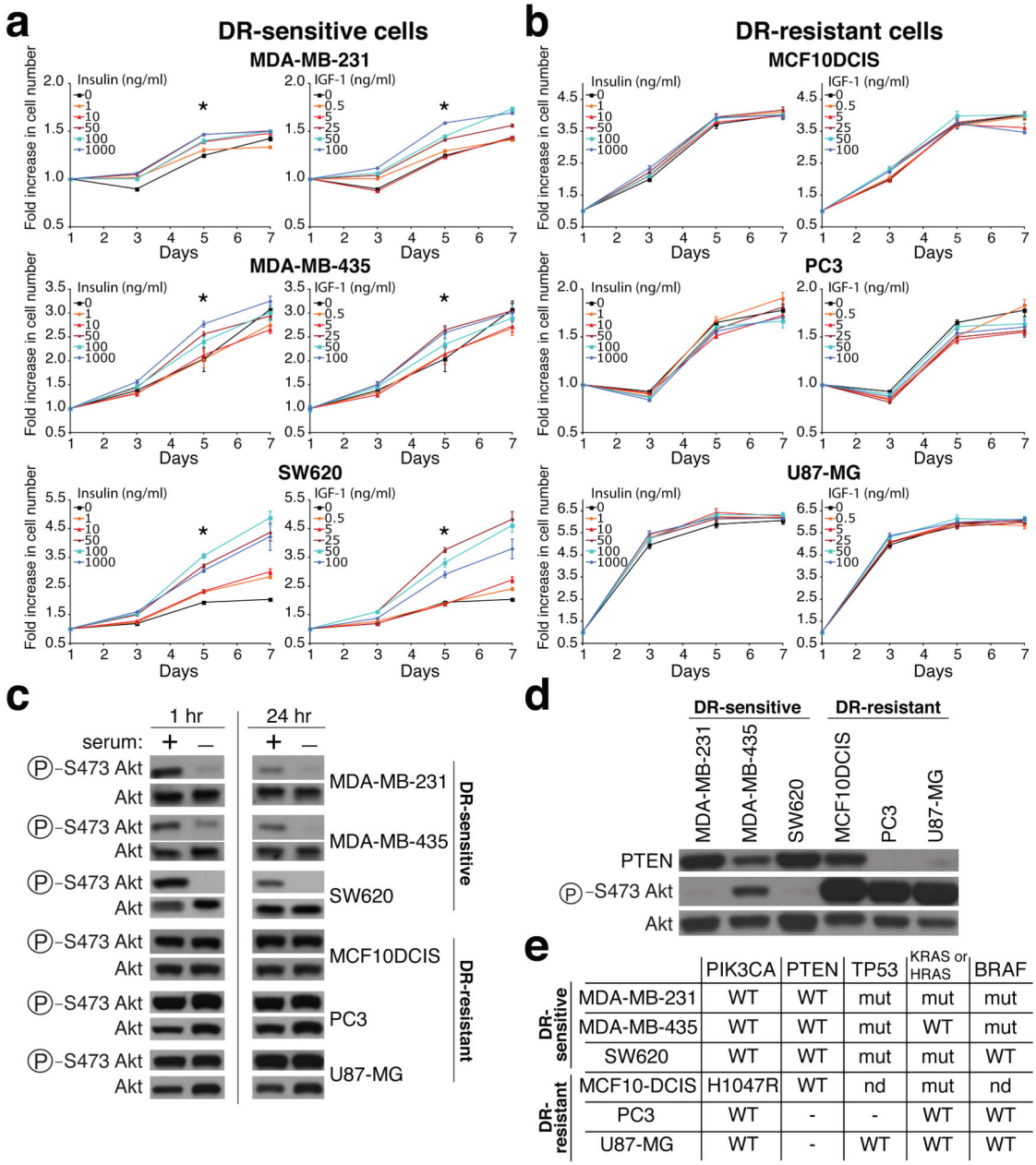


e

| | | PIK3CA | PTEN | TP53 | KRAS or HRAS | BRAF |
|---|---|---|---|---|---|---|
| DR-sensitive | MDA-MB-231 | WT | WT | mut | mut | mut |
| | MDA-MB-435 | WT | WT | mut | WT | mut |
| | SW620 | WT | WT | mut | mut | WT |
| DR-resistant | MCF10-DCIS | H1047R | WT | nd | mut | nd |
| | PC3 | WT | - | - | WT | WT |
| | U87-MG | WT | - | WT | WT | WT |

**Figure 2. Constitutive PI3K activation correlates with tumour resistance to DR**

**a**,**b,** Proliferation curves of cancer cells that form DR-sensitive (a) and DR-resistant (b) tumours cultured in the presence of increasing concentrations of insulin or IGF-1. Data points represent means ± s.e.m for n = 6. * indicates $P \leq 0.001$ for differences between 0 ng/ml and 1000 ng/ml insulin or 0 ng/ml and 100 ng/ml IGF-1 at day 5. **c**, Phospho-S473 Akt and total Akt levels in cells grown in the presence or absence of serum for 1 or 24 hours. **d**, PTEN expression, phospho-S473 Akt and total Akt levels in the different cell lines. **e**, Sequencing results for *PIK3CA* hot-spot mutations, loss of or mutational status of *PTEN*, *TP53*, *RAS* and *BRAF* in all cell lines studied. WT refers to wild-type; mut to mutant, and nd to not determined. "–" indicates absence of the gene.

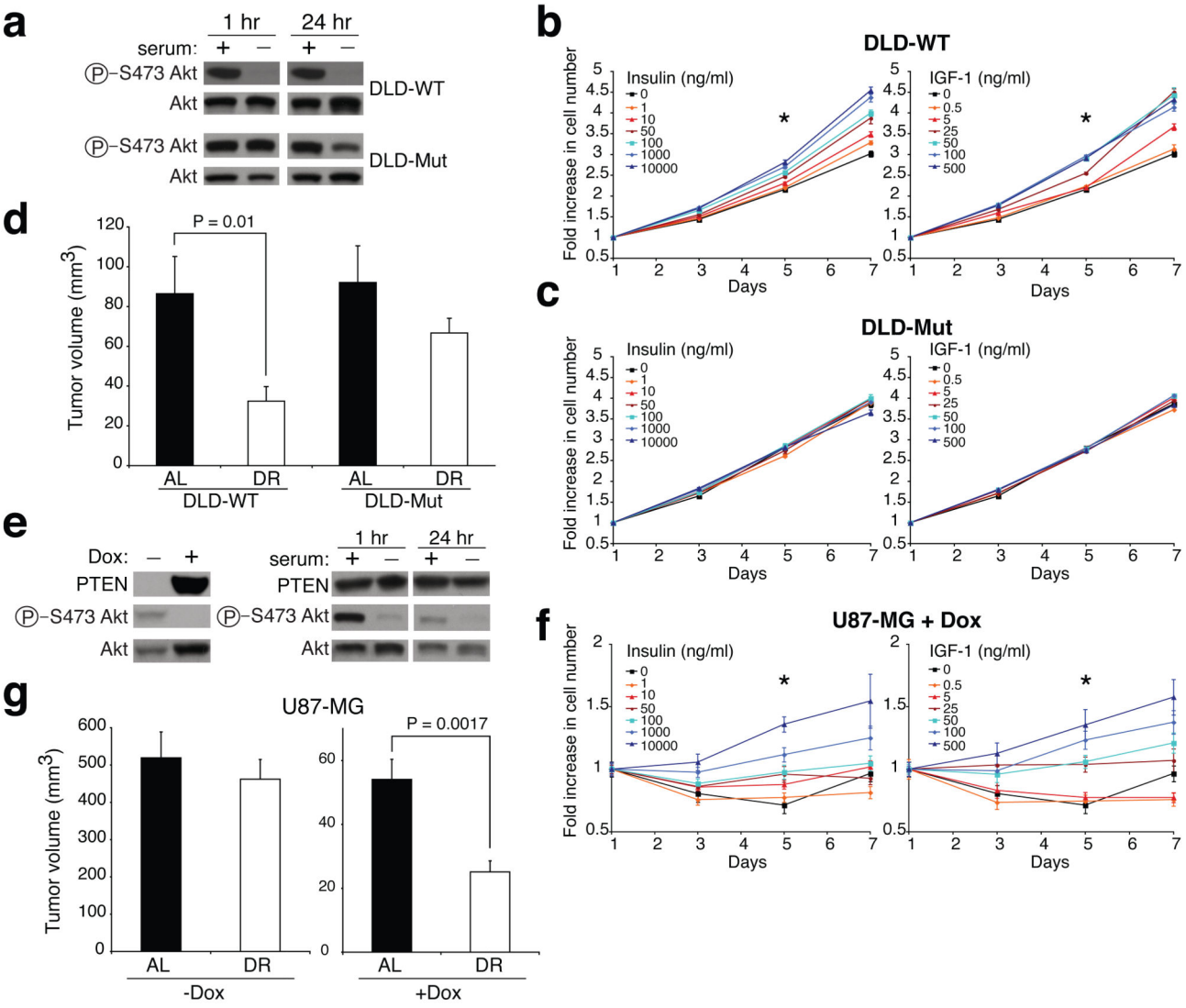


**Figure 3. PIK3CA activating mutations or PTEN loss suppress tumour sensitivity to DR**

**a**, Phospho-S473 Akt and total Akt levels in DLD-WT and DLD-Mut cells in the presence or absence of serum for 1 or 24 hours. **b**, **c**, and **f**, Proliferation curves of DLD-WT, DLD-Mut, and doxycycline(Dox)-treated (1μg/ml) U87-MG cells in the presence of increasing concentrations of insulin or IGF-1, n=6. * indicates P ≤ 0.001 as in Fig. 2a, b. **d**, Volumes of DLD-WT and DLD-Mut tumours in AL or DR mice (n= 7–10). **e**, PTEN, phospho-S473 Akt and total Akt levels in U87-MG cells in the presence or absence of Dox (left panel) and in Dox-treated U87-MG cells in the presence or absence of serum for 1 hour or 24 hours (right panel). **g**, Volumes of U87-MG tumours in AL and DR mice administered drinking water with or without Dox (n= 7–9). Data in **b**, **c, d**, **f** and **g** represent means ± s.e.m.

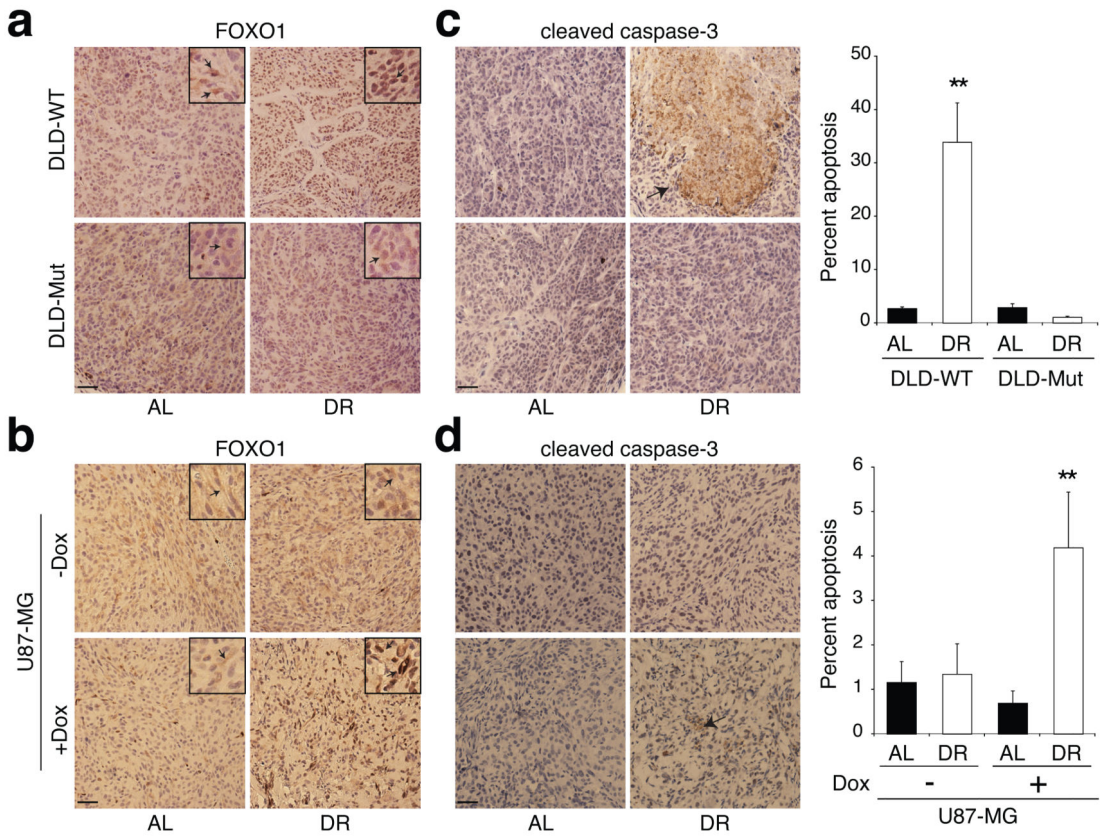


**Figure 4. Effects of modulation of PI3K signaling on the apoptotic response of tumours to DR**

**a-d**, Immunohistochemical analyses of FOXO1 (a, b) and cleaved caspase-3 (c, d) in tumours formed by DLD-WT and DLD-Mut cells and by the PTEN-inducible U87-MG cells in mice treated or non-treated with doxycycline (Dox). Graphs to right of images indicate percent of total cells that are positive for cleaved caspase-3. Data in **c** and **d** graphs are means ± s.e.m, measured in 9 images (1000 nuclei counted per image) from 3 different tumours per group. ** indicates $P \leq 0.01$. All images were acquired at the same magnification and scale bar = 20 μm. Framed inserts in **a** and **b** are a 3.9-fold magnification of a representative area of the corresponding larger image. Arrows point to immunoreactivity for FOXO1 (a, b) or cleaved caspase-3 (c and d).

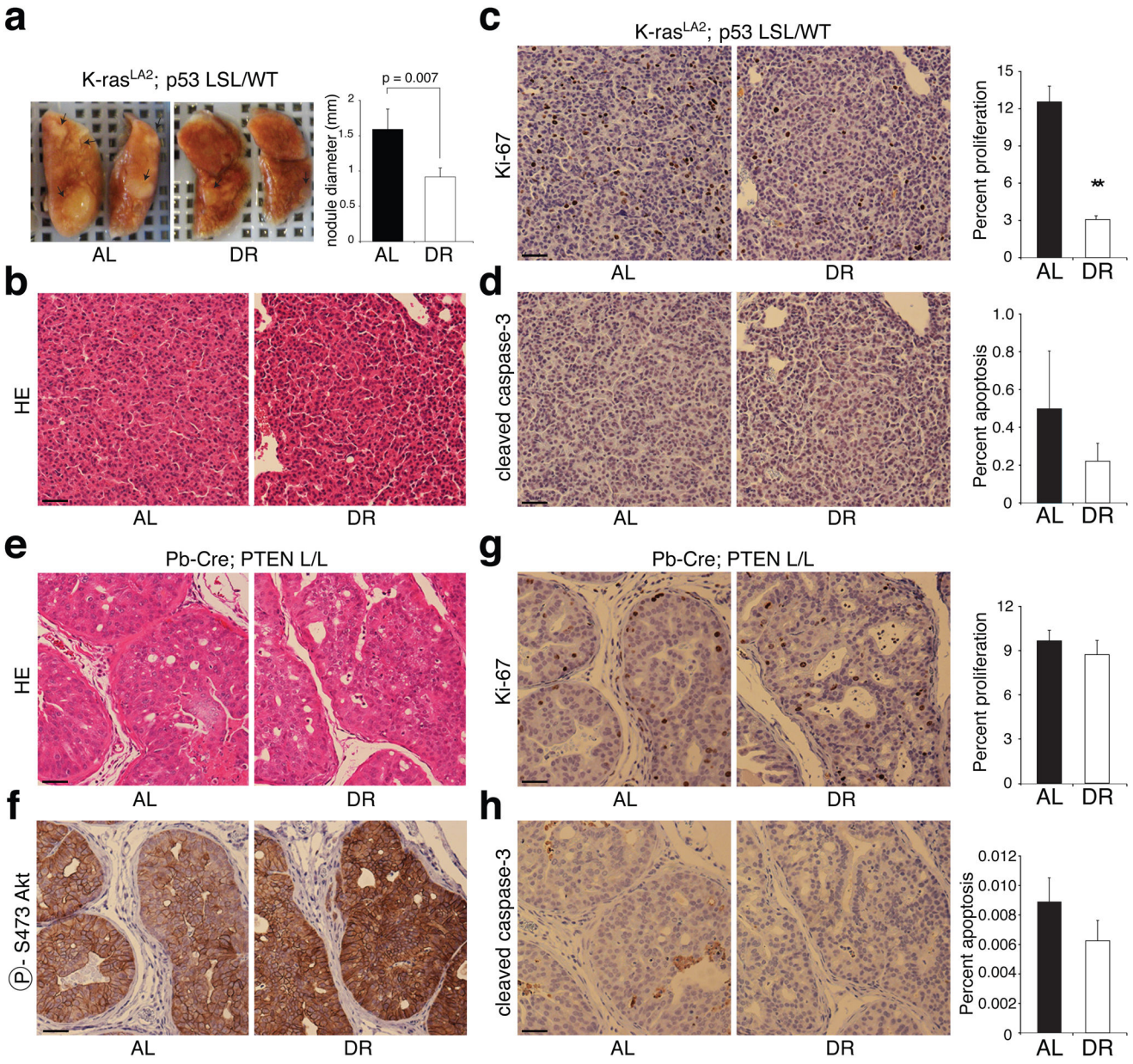


**Figure 5. A K-RAS mouse model of lung cancer but not a *PTEN*-null model of prostate cancer is sensitive to DR**

**a**, Representative images of lungs and average diameter of tumour nodules on the surface of the lungs (graph) of 7-week-old *K-RAS$^{LA2}$; P53 LSL/ WT* mice under AL or DR conditions (n=3). **b-d**, H&E staining (b) and immunohistochemical analyses of Ki-67 (c) and cleaved caspase-3 (d) in sections prepared from lungs in **a**. **e-h**, H&E staining (e) and immunohistochemical analyses of phospho-Akt S473 (f), Ki-67 (g), and cleaved caspase-3 (h) in prostates of 11-week-old *Probasin-Cre; PTEN L/L* mice under AL or DR conditions. In **c, d, g, and h**, graphs to right of respective images indicate percent of total cells that are positive for Ki-67 or cleaved caspase-3. Graphs show means ± s.e.m. of percent of proliferating (c and g) or apoptotic cells (d and h) measured in 10 images (1000 nuclei

counted per image) from 2 different tumours per group. All pictures were captured under the same magnification and scale bar = 20 μm. ** indicates $P = 8.3 \times 10^{-8}$.